CERAMIC TILES WITH HIGH IONISING RADIATION ATTENUATION

Guaita, L.(1), Bengochea, M.A.(1), Lucas, F.(2), Flors, Mª.R.(2),

Boix, J.(3), Aguilella, M.(3), Orts, Mª.J.(3), Mestre, S.(3),

(1) Keraben Grupo, S.A.

(2) Kerafrit, S.A

(3) Instituto de Tecnología Cerámica (ITC). Asociación de Investigación de las Industrias Cerámicas (AICE), Universitat Jaume I. Castellón. Spain.

1. ABSTRACT

In this study, ceramic tiles were developed that are capable of absorbing ionising radiation, in particular X-rays, in the range of energies used in X-ray diagnostic equipment. These tiles constitute an alternative construction element to current solutions based on the incorporation of sheets of lead or plasterboards containing barites as radiation shielding, in radiology services, dental clinics, veterinary clinics, research centres, industrial facilities that use X-rays, etc.

The manufacturing process differs from that of conventional ceramic tiles because of the incorporation into the ceramic body formulation of more than 50 wt% frit, containing lead bisilicate, bismuth, or barium. This yields a product with a mixed glassy and crystalline mineralogy characterised by sufficiently low leaching to enable the product to be classified, at the end of its service life, as non-hazardous or even inert waste, depending on the elements it contains.

2. INTRODUCTION

Lead is a soft, stable metal with high ductility and a low melting temperature (327,4°C), leading to use in a great number of applications dating back to antiquity. One lead characteristic, owing to its high atomic number, is the protection it provides against ionising radiation and consequent use in the protective clothing (aprons, gloves, etc.) of healthcare workers and in X-ray room walls. In fact, lead is at present possibly the most widely used X-ray shielding material. Lead is used both in the form of sheeting or blocks and as particles dispersed in a polymer(1). Glasses with a high PbO content are used in special applications (X-ray room windows), these being very expensive products. Other lead-containing materials are $BaPbO_3$, used in preparing composites, with polymers or with aluminium, or Pb- and Ba-containing phosphorus glasses(2).

Steel and common concrete(3) are also used as shielding, but they need to be incorporated into the design of the building that is to lodge the X-ray source, it being quite complicated to install them in an already constructed building, owing to the relatively high required thicknesses. When a room containing an X-ray source is to be shielded, the simplest option is to cover the floor, walls, and ceiling with a highly absorbent material, for a coating thickness to be acceptable, as well as easy to install and, where appropriate, remove. The most widely used option at present is the installation of lead sheeting as shielding in X-ray rooms. However, when it comes to refurbishment or demolition, lead wastes must be handled with special care, owing to the ease with which lead solubilises in slightly acid mediums, thus readily entering aquifers and subsequently passing on to living beings, causing lead poisoning.

In view of such risks, widespread research has been conducted to identify alternative materials for ionising radiation shielding. The materials containing elements with a high atomic number, such as Ba, W, and Bi, have obviously drawn most attention(4).

Barium is a good X-ray absorber and barium-based commercial products have thus been developed. Possibly the best known are concretes with barite(5),(6) or plasterboards containing barites (combining calcium sulphate with barium sulphate), and resembling common gypsum plasterboards used in building. Since barium compounds exhibit a certain toxicity, products containing these need to be installed with all due precaution and the waste must be appropriately handled. In addition to commercial products, other less well-known materials have been reported: ceramic tiles containing barium in the form of celsian (barium aluminosilicate), and silicate or borosilicate glasses containing this in their composition(7),(8). In the case of tungsten, epoxy resin and WO_3 nanoparticle composites have been studied as shielding materials(9). With regard to Bi, this has been studied as shielding in the form of silicate(10), borate(11),(12) or bismuth borosilicate(13) glasses that can optionally incorporate other absorber elements such as Ba or Pb(14).The main advantage of bismuth is the absence of toxicity; however, it is very expensive compared to other elements.

This study was undertaken to develop an alternative X-ray shielding material in the form of a ceramic tile, which was therefore easy to install and remove, and provided numerous aesthetic possibilities.

The developed tiles contain an important quantity of one or more frits (insoluble silica glass), bearing the radiation-absorbing elements (Pb, Ba, and Bi). These frits, together with the natural raw materials (clays, quartz, etc.), can be processed in conventional ceramic plants to obtain a product with technical and aesthetic properties similar to those of ceramic tiles, while displaying a great X-ray absorption capability. As waste the developed ceramic tiles have a non-hazardous or inert character, providing a significant advantage compared to shielding based on metallic lead sheets.

3. MATERIALS AND PROCEDURE

3.1. PREPARATION OF TEST PIECES

Mixtures of raw materials (clays, kaolins, and feldspars) and frits containing one of the X-ray shielding capability-contributing elements (Pb, Bi, Ba) were prepared. The mixtures, with different frit contents, were wet milled and spray dried in the laboratory. They were then milled for different times to determine the effect of particle size. Test pieces measuring 10 cm x 5 cm were formed from the resulting mixtures in a laboratory press. Pressing pressure was 300 $kg \cdot cm^{-2}$ and press powder moisture content was 0.055 kg water/kg dry solid. The effect of test piece thickness on the material's X-ray shielding capability was studied by preparing series of test pieces 7, 8.5 and 10 mm thick. After the laboratory pieces had been dried they were fired in an electric laboratory kiln at different maximum temperatures, from 800 to 950°C. Once the optimum processing conditions had been established, pieces were obtained on an industrial scale.

In the course of the study, different compositions with mixtures of different radiation-attenuating elements were used, added to a standard ceramic floor tile body. The present study describes the results of the composition without any attenuating elements and of the compositions with a single attenuating element added to the ceramic body (see Table 1)

Ref.	PbO (%)	BaO (%)	Bi_2O_3 (%)
A	37	-	-
B	-	37	-
C	-	-	37
C	-	-	-

Table 1: *Studied samples and attenuating element content (% by weight of oxide)*

3.2. DETERMINATION OF SOLUBILITY

Semi-quantitative analysis by wavelength-dispersive X-ray fluorescence spectrometry (using reference materials that assured measurement traceability) was performed to identify the elements present in the samples. The potentially hazardous elements contained in each sample were thus determined, those elements being selected that needed to be analysed for classification according to the Council Decision of 19 December 2002, establishing criteria and procedures for acceptance of waste at landfills, pursuant to Article 16 and Annex II to Directive 1999/31/EC. These regulations establish three types of waste: inert waste, non-hazardous waste, and hazardous waste, as well as criteria for acceptance of these wastes at different landfills. The criteria are based on the determination of certain element concentrations in the resulting leachate after continuously stirring the waste in water at a liquid/solid ratio of 10 $L \cdot kg^{-1}$.

The leaching tests were conducted according to standard UNE-EN 12457-2:2003. The sample was ground to a particle size below 4 mm, after which 0.090 ± 0.005 kg of the ground sample was weighed and mixed in 0.90 ± 0.05 kg distilled water. The mixture was continuously stirred for 24 hours at room temperature. The liquid fraction was then separated by filtration under vacuum through a filter of 0.2 μm pore size. Pb and Ba were analysed in the resulting solution with an atomic absorption (AA) spectrophotometer. In the samples where the value obtained was beneath the detection limit of the AA instrument, lead was determined with an Agilent 7500CX ICP-MS instrument, with collision cell.

3.3. DETERMINATION OF THE SHIELDING CAPABILITY

3.3.1. MEASUREMENT OF X-RAY MASS ABSORPTION

The shielding capability of the developed materials was evaluated using an inspection instrument for bulk density measurement by X-ray absorption, which functions according to the Lambert-Beer law (Eq. 1). According to this law, when an ionising radiation crosses a given material medium, the fraction of incident radiation that is absorbed by the material depends exclusively on its chemical nature, its thickness, and its bulk density.

$$\frac{I}{I_0} = e^{-\mu h \rho} \qquad \text{(Eq.1)}$$

Eq. 1 represents the Lambert-Beer law applied to a monochromatic radiation and to a perfectly homogeneous material throughout its thickness, where I_0 is incident radiation intensity, I transmitted radiation intensity, h thickness of the material, ρ bulk density, and μ the mass absorption coefficient for the radiation wavelength.

That is, if a material's bulk density and thickness are known, its mass absorption coefficient can be determined from the quantity of absorbed energy. In practice, however, Eq. 1 is only approximate because the X-ray tubes customarily used to perform this type of test emit polychromatic radiation and the analysed materials are usually not homogeneous. This significantly complicates the relationships between the transmitted radiation intensity and the X-ray absorption coefficient, which depends on incident radiation wavelength.

Although a material's absorption coefficient can be calculated from its chemical composition and the radiation spectrum, the simplest approach is to obtain an empirical relationship between the material's bulk density, its thickness, and the resulting radiation attenuation when the radiation crosses it, as was done in this study.

Figure 1 schematically illustrates the operation of the instrument used in determining the X-ray absorption mass coefficients. The piece to be characterised (1) was placed flat on the conveyor belt (see Figure 2) and it travelled towards the head where the telemetry system (2) for measuring piece thickness, the X-ray emitter tube (3), and the radiation sensor (4) were installed. The head moved at right angles to the travelling piece, performing a complete scan. During the tests the measuring system performed successive scans from right to left, at a maximum rate of 1000 mm/s, with a minimum vertical movement between lines of 1 mm. While it moved, the device took measurements of piece thickness and of the radiation intensity transmitted through the piece, with a sampling frequency of 10 readouts per millimetre.

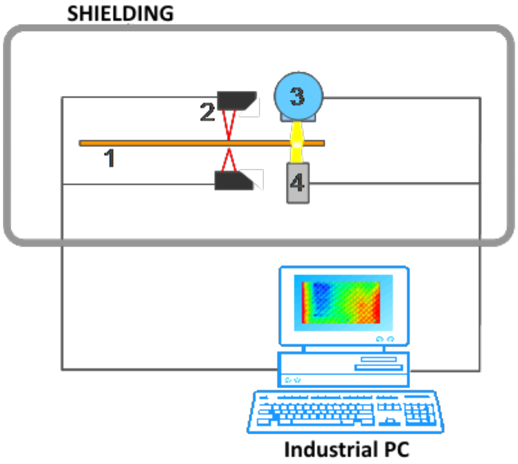

Figure 1. *Operating scheme of the instrument for bulk density measurement by X-ray absorption.*

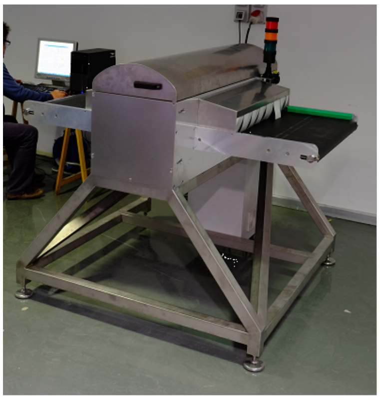

Figure 2. *General view of the set-up used in measuring the mass absorption coefficient.*

3.3.2. CALCULATION OF THE EQUIVALENT THICKNESS OF LEAD

A widely used variable in radiation protection, with regard to shielding calculations, is the equivalent thickness of lead. This parameter indicates how many millimetres of a given material are needed to equal the shielding provided by 1 millimetre of pure metallic lead. For example, 22 mm AISI 304 steel are equivalent to 1 mm Pb at 100 keV of incident X-radiation.

To theoretically calculate the equivalent lead thickness of a material, the Lambert-Beer law can be used, which adopts the form of Eq. 2, for the material characterised, and the form of Eq. 3 for lead. Setting these two equations equal readily yields Eq. 4, which allows the equivalent thickness of lead (h_{Pb}) to be calculated for a given thickness of the studied material (h_M) from the density of lead (ρ_{Pb}) and of the material (ρ_M) and of their respective mass absorption coefficients (μ_{Pb} and μ_M).

$$\left.\begin{array}{ll}\left(\dfrac{I}{I_0}\right)_{MATERIAL} = \exp(-\mu_M.\rho_M.h_M) & \text{(Eq.2)} \\ \left(\dfrac{I}{I_0}\right)_{LEAD} = \exp(-\mu_{Pb}.\rho_{Pb}.h_{Pb}) & \text{(Eq.3)}\end{array}\right\} \Rightarrow h_{Pb} = h_M.\frac{\mu_M.\rho_M}{\mu_{Pb}.\rho_{Pb}} \quad \text{(Eq.4)}$$

The mass attenuation coefficient of the material can be obtained either experimentally or theoretically from Eq. 5. This equation calculates the mass attenuation coefficient of a composite material (μ_M) from the attenuation coefficients of its compositional elements (μ_i) and its mass fractions (w_i). The National Institute of Standards and Technology (NIST)(15) tabulates the mass attenuation coefficients of all elements in the periodic table, for different wavelengths of incident monochromatic radiation.

$$\mu_M = \sum_{i=1}^{n} \mu_i.w_i = \mu_1.w_1 + \mu_2.w_2 + \ldots + \mu_n.w_n \quad \text{(Eq.5)}$$

The main difficulty involved using a mass attenuation coefficient obtained experimentally with the device described in section 3.3.1 to calculate the equivalent thickness of lead stemmed from the fact that the X-ray tube radiation was polychromatic. Indeed, an X-ray beam is characterised by the quantity of photons present in the beam or intensity and by their penetrating capability or quality. The quality of the beam, i.e. the photon energy distribution, depends on the maximum or peak voltage applied to the tube and on the presence or absence of filters in the instrument configuration. If the applied voltage is 100 kV, for example, its peak kilovoltage is 100 kVp. The maximum photon energy in the beam will be 100 keV, but only a small percentage of the emitted X-rays will have this energy and most will have lower energy, according to a continuous distribution(16).This peculiarity, together with the fact that the X-ray tube of the inspection instrument used had a peak voltage of 80 kVp, led to choosing the theoretical procedure to calculate the equivalent thicknesses of lead at voltages >80 kVp of the studied materials.

4. RESULTS AND DISCUSSION

4.1. WASTE CLASSIFICATION ACCORDING TO UNE-EN 12457-2:2003

The semi-quantitative chemical analyses indicated that the only elements to be considered for classification as waste in the synthesised samples were Pb in sample A and Ba in sample B. The leaching test was therefore only conducted on these samples. The test results and their comparison with the allowable limits according to Directive 1999/31/EC are detailed in Table 2.

Element	Concentration in the leachate ($mg \cdot kg^{-1}$)		Allowable limits for landfills ($mg \cdot kg^{-1}$)		
	Sample A	Sample B	Inert	Non-hazardous	Hazardous
Pb	7.3	-	0.5	10	50
Ba	-	1360	20	100	300

Table 2. *Leaching results in the studied samples and allowable limits.*

The results indicate that the tiles in sample A would be deemed non-hazardous waste on ending their service life. However, on optimising processing conditions, pieces were obtained with Pb that would be rated as inert waste. In contrast the tiles in sample B would be deemed hazardous waste, so that their composition would need to be reformulated to reduce Ba leaching. As sample C contained no element included in Directive 1999/31/EC, it would be considered inert waste.

4.2. SHIELDING CAPABILITY

Following the procedure described in section 3.3, the mass absorption coefficients of the studied compositions were experimentally determined, working at the maximum power of the X-ray tube used (80 kVp and 1.2 mA). Three test pieces with a similar density and different thickness of each composition were analysed at the same time, with a view to obtaining the mass attenuation coefficient by fitting the Lambert-Beer law. Figure 3 shows the placement of samples of compositions A, B, and C at the entry of the inspection instrument, before characterisation.

Figure 3: *Placement of the pieces at the entry of the inspection instrument*

By way of example, Figure 4 shows the results obtained for sample A with the measuring instrument. The thickness distributions from the signal generated by the X-ray sensor and the calculated bulk density of the three test pieces are depicted in the false-colour images. The average value of each parameter analysed is shown below each image. It may be observed that, as was to be expected, the lower the thickness of the test piece, for the same composition and bulk density, the higher was the transmitted radiation.

Figure 5 shows a plot of the fits of the logarithm of intensity (expressed as photodiode signal in V) versus the product of bulk density by thickness of the analysed compositions. The slope of each straight line corresponded to the mass attenuation coefficient μ according to the Lambert-Beer law.

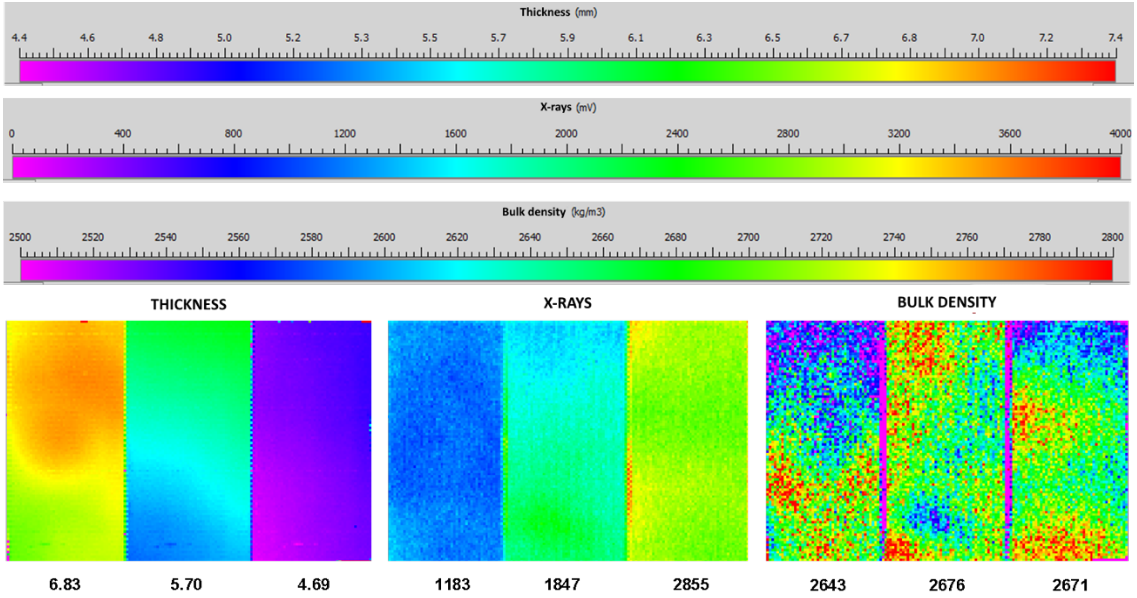

Figure 4. *Results obtained by the X-ray inspection instrument for sample A.*

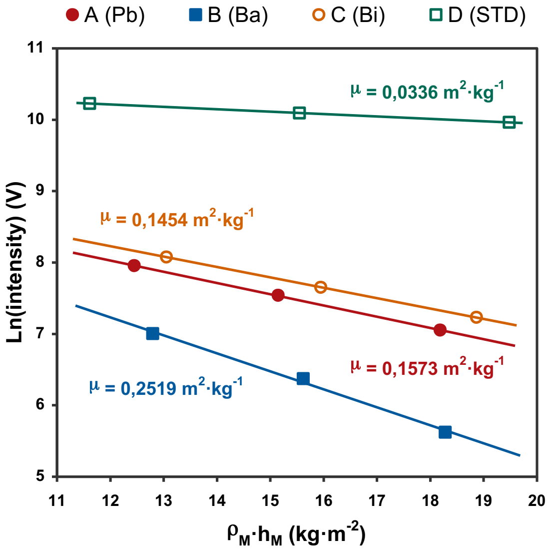

Figure 5: *Variation of transmitted radiation intensity versus the product of density by thickness.*

It may be observed that the composition with barium oxide (ref. B) displayed the highest attenuation coefficient for the studied irradiation quality, followed by lead oxide (ref. A) with a 37.6% lower attenuation coefficient and bismuth oxide (ref. C), with a 42.3% lower coefficient with respect to barium oxide. On the other hand, the sample with 37% BaO displayed a 7.5 times higher attenuation coefficient to the standard porcelain tile composition used as starting composition in making the samples.

To better understand the results obtained, Figure 6 shows plots of the mass attenuation coefficient according to the irradiation energy for elemental lead, barium, and bismuth. It may be observed that in the stretch between about 40 keV and 90 keV, the mass attenuation coefficient of barium was higher than that of lead. Above 90 keV, the plot corresponding to lead exhibited a sharp discontinuity (an absorption edge) and its attenuation coefficient became higher than that of barium until it reached 1 MeV, at which they had practically the same attenuation.

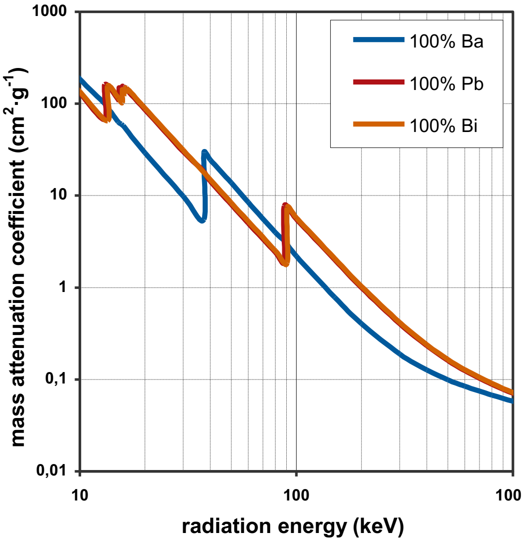

Figure 6: *Attenuation coefficients versus radiation energy*$^{(16)}$.

This indicated that the barium oxide-based composition exhibited higher shielding values than the lead oxide-based composition, owing to the quality of the radiation used in the tests. If the material were to be used as shielding against greater incident energy, lead oxide would provide greater attenuation than barium oxide.

With regard to bismuth oxide, its attenuating power was similar to that of lead oxide. This outcome, in addition to the very high cost of bismuth-bearing raw materials, advises against using it as attenuating material in these compositions, provided leaching-stabilised lead- or barium-based compositions can be developed.

4.3. EQUIVALENT THICKNESS OF LEAD

The equivalent lead thickness of the studied samples was calculated according to the methodology set out in section 3.3.2. To calculate the mass attenuation coefficients of the materials (μ_M), the chemical analyses conducted and the theoretical mass attenuation coefficients provided by the NIST were used. The calculations were made at an incident radiation energy of 100 keV, which encompasses the techniques commonly used in X-ray diagnostics. For comparative purposes, the mass attenuation coefficients of other materials were also calculated.

Table 3 details the mass attenuation coefficient of each material at an incident radiation of 100 keV, bulk density, and the calculation of the thickness of the material needed to obtain the same attenuation as that of 1 mm metallic lead.

Material	μ_m ($m^2 \cdot kg^{-1}$)	ρ_m ($kg \cdot m^{-3}$)	e_m (mm)	Material	μ_m ($m^2 \cdot kg^{-1}$)	ρ_m ($kg \cdot m^{-3}$)	e_m (mm)
Lead	0.5549	11340	1	Sample B	0.0964	2600	25
Bronze SAE-40	0.0702	8820	10	Sample D	0.0301	2350	89
Sample A	0.2214	2650	11	STD concrete	0.0271	2300	101
Sample C	0.2214	2700	11	Red brick	0.0284	1700	131
Concrete containing barites	0.1127	3350	17	Plaster	0.0193	840	389
ANSI 304 steel	0.0368	7930	22	Wood	0.0162	650	600

Table 3: *Theoretical mass attenuation coefficient and thickness of the material equivalent to 1 mm lead at 100 KeV.*

Sample A (PbO) and sample C (Bi_2O_3) provided the same attenuation coefficient as their bulk density was very similar. The thickness of material to equal a shield of 1 mm lead was 11 mm for both samples. Owing to the current high price of bismuth and the low leaching values of the lead-containing samples, it would be advisable to use lead oxide in industrial pieces. It may be observed that in the case of sample B (BaO), at an incident radiation energy of 100 keV, 25 mm material would be needed to equal 1 mm lead. In the case of sample D (STD), without any type of attenuating component, a thickness of 89 mm would be required.

5. CONCLUSIONS

In this study, ceramic tiles were developed for use in construction solutions as X-ray shielding in X-ray diagnostic facilities, based on a composition made up of natural raw materials and frits containing radiation-attenuating elements.

The frits allowed several attenuating elements to be incorporated, which improved tile response to different incident radiation energies. Thus, at low energies, Ba was very effective while at energies above 90 keV, lead and bismuth exhibited greater radiation attenuation.

The ceramic tile attenuation capability was very high, as the active element (Lead – Bismuth – Barium) content exceeded 35 wt%. In the most favourable case, an 11-mm-thick tile was equivalent to a 1-mm-thick lead sheet at 100 keV.

Of the three tested absorber elements, Ba was the only element that generated tiles which would be deemed hazardous waste with the tested composition. In contrast, the Pb-containing tile exhibited lead leaching that, in accordance with Article 16, Annex II of Directive 1999/31/EC, allowed it to be classified as non-hazardous or inert waste, depending on the processing conditions used. This characteristic would entail elimination of the risk involved in handling lead sheets at the end of a facility's service life. Finally, the tile that contained Bi would be classified as inert waste, though the high cost of Bi could limit its use.

The ceramic tiles could be installed on an already existing substrate and would provide a wide range of aesthetic possibilities. In addition, the tile shield thickness was lower than that of alternative solutions based on concrete walls or special gypsum plasterboards.

REFERENCES

[1] Weir, D.; Hare, J.T.; (1996). Radiation shielding material. US Patent 5525408.

[2] Kharita, M.H.; Jabra, R.; Yousef, S.; Samaan, T. (2012). Shielding properties of lead and barium phosphate glasses. Radiation Physics and Chemistry. 81:1568–1571.

[3] Kurudirek, M.; Özdemir, Y.; Simsek, Ö; Durak, R. (2010). Comparison of some lead and non-lead based glass systems, standard shielding concretes and commercial window glasses in terms of shielding parameters in the energy region of 1 keV–100 GeV: A comparative study. Journal of Nuclear Materials 407: 110-115.

[4] McCaffrey, J.P.; Shen, H.; Downton, B.; Mainegra-Hing, E. (2007). Radiation attenuation by lead and nonlead materials used in radiation shielding garments. Med. Phys. 34(2): 530-537.

[5] Bekir Topçu, I. (2003). Properties of heavyweight concrete produced with barite. Cement and Concrete Research. 33:815–822.

[6] Akkurt, I.; Akyıldırım, H.; Mavi, B.; Kilincarslan, S.; Basyigit, C. (2010). Photon attenuation coefficients of concrete includes barite in different rate. Annals of Nuclear Energy. 37:910–914.

[7] Amritphale, S.S.; Anshul, A.; Chandra, N.; Ramakrishnan, N. (2007). Development of celsian ceramics from fly ash useful for X-ray radiation-shielding application. Journal of the European Ceramic Society .27: 4639–4647.

[8] Tuscharoen, S.; Kaewkhao, J.; Limkitjaroenporn, P.; Limsuwan, P.; Chewpraditkul, W. (2012). Improvement of BaO:B_2O_3:Fly ash glasses: Radiation shielding, physical and optical properties. Annals of Nuclear Energy 49:109–113.

[9] Noor Azman, N.Z.; Siddiqui, S.A.; Lowa, I.M. (2013). Characterisation of micro-sized and nano-sized tungsten oxide-epoxy composites for radiation shielding of diagnostic X-rays. Materials Science and Engineering. C33:4952–4957.

[10] Singh, K.J.; Sandeep Kaur; Kaundal, R.S. (2014). Comparative study of gamma ray shielding and some properties of $PbO–SiO_2–Al_2O_3$ and $Bi_2O_3–SiO_2–Al_2O_3$ glass systems. Radiation Physics and Chemistry 96:153–157.

[11] Kaewjaenga, S.; Kaewkhaob, J.; Limsuwanc, P.; Maghanemia, U. (2012). Effect of BaO on Optical, Physical and Radiation Shielding Properties of SiO_2-B_2O_3-Al_2O_3-CaO-Na_2O Glasses System. Procedia Engineering. 32:1080–1086

[12] J. Kaewkhao, J.; Pokaipisit, A.; Limsuwan, P. (2010). Study on borate glass system containing with Bi_2O_3 and BaO for gamma-rays shielding materials: Comparison with PbO. Journal of Nuclear Materials 399: 38–40.

[13] Chanthima, N.; Kaewkhao , J. (2013) Investigation on radiation shielding parameters of bismuth borosilicate glass from 1 keV to 100 GeV. Annals of Nuclear Energy 55: 23–28

[14] Kirdsiri, K.; Kaewkhao, J.; Chanthima, N.; Limsuwan, P. (2011). Comparative study of silicate glasses containing Bi_2O_3, PbO and BaO: Radiation shielding and optical properties. Annals of Nuclear Energy 38:1438–1441.

[15] http://www.nist.gov/pml/data/xraycoef/

[16] http://www.uco.es/~fa1orgim/fisica/archivos/Radiacciones/ER$12AMR.pdf